Handling Long and Richly Constrained Tasks through Constrained Hierarchical Reinforcement Learning

Yuxiao Lu¹, Arunesh Sinha², Pradeep Varakantham¹

¹Singapore Management University

²Rutgers University
yxlu.2021@phdcs.smu.edu.sg, arunesh.sinha@rutgers.edu, pradeepv@smu.edu.sg

Abstract

Safety in goal directed Reinforcement Learning (RL) settings has typically been handled through constraints over trajectories and have demonstrated good performance in primarily short horizon tasks. In this paper, we are specifically interested in the problem of solving temporally extended decision making problems such as robots cleaning different areas in a house while avoiding slippery and unsafe areas (e.g., stairs) and retaining enough charge to move to a charging dock; in the presence of complex safety constraints. Our key contribution is a (safety) Constrained Search with Hierarchical Reinforcement Learning (CoSHRL) mechanism that combines an upper level constrained search agent (which computes a reward maximizing policy from a given start to a far away goal state while satisfying cost constraints) with a low-level goal conditioned RL agent (which estimates cost and reward values to move between nearby states). A major advantage of CoSHRL is that it can handle constraints on the cost value distribution (e.g., on Conditional Value at Risk, CVaR) and can adjust to flexible constraint thresholds without retraining. We perform extensive experiments with different types of safety constraints to demonstrate the utility of our approach over leading approaches in constrained and hierarchical RL.

1 Introduction

Reinforcement Learning (RL) is a framework to solve decision learning problems in environments that have an underlying (Partially Observable) Markov Decision Problem, (PO-)MDP. Deep Reinforcement Learning (François-Lavet et al. 2018; Hernandez-Leal, Kartal, and Taylor 2019) approaches have been shown to solve large and complex decision making problems. For RL agents to be relevant in the day-to-day activities of humans, they need to handle a wide variety of temporally extended tasks while being safe. A few examples of such multi-level tasks are: (a) planning and searching for valuable targets by robots in challenging terrains (e.g., disaster areas) while navigating safely and preserving battery to reach a safe spot; (b) for autonomous electric vehicles to travel long distances in minimum time, they need to optimize the position of recharge locations along the way to ensure the vehicle is not left stranded; (c) cleaning robots to clean a house while avoiding slippery and unsafe

Copyright © 2024, Association for the Advancement of Artificial Intelligence (www.aaai.org). All rights reserved.

areas (e.g., stairs) and retaining enough charge to move to a charging dock. The following key challenge needs to be addressed in the above mentioned problems of interest:

Computing an execution policy that satisfies safety constraints (in expectation or in a confidence bounded way) for temporally extended decision making problems in the presence of uncertainty.

Existing research in temporally extended decision making problem has focused on hierarchical RL methods (Nachum et al. 2018; Zhang et al. 2020; Kim, Seo, and Shin 2021; Levy et al. 2017). These approaches successfully solve long horizon tasks mainly in the widely applicable setting of goal conditioned RL (Liu, Zhu, and Zhang 2022), but they are unable to deal with safety constraints. On the other hand, most existing research in handling trajectory based safety constraints has focused on constrained RL approaches (Simão, Jansen, and Spaan 2021; Gattami, Bai, and Aggarwal 2021), where constraints are enforced on expected cost. A recent method that has considered percentile/confidence based constraints is WCSAC (Yang et al. 2021). Unfortunately, these constrained RL approaches are typically only able to solve short horizon problems where the goal is not too far away. We address the need to bring together these two threads of research on hierarchical RL and constrained RL, which have mostly progressed independently of each other (Roza, Roscher, and Günnemann 2023). To that end, we propose a new Constrained Search with Hierarchical Reinforcement Learning (CoSHRL) approach, where there is a hierarchy of decision models: (a) The lower level employs goal conditioned distributional RL to learn reward and cost distributions to move between two local states that are near to each other. (b) The upper level is a constrained search mechanism that builds on Informed RRT* (Gammell, Srinivasa, and Barfoot 2014) to identify the best waypoints to get from a given start state to a "far" away goal state. This is achieved while ensuring overall expected or percentile cost constraints (representative of robust safety measures) are enforced.

Contributions: Our key contributions are: (1) we provide a *scalable constrained* search approach suited for *long horizon tasks* within a hierarchical RL set-up, (2) we are able to handle rich *percentile* constraints on cost distribution, (3) the design of enforcing the constraints at the upper-level search

allows *fast recomputation* of policies in case the constraint threshold or start/goal states change, and (4) *mathematical guarantee* for our constrained search method. Finally, we provide an extensive empirical comparison of CoSHRL to leading approaches in hierarchical and constrained RL.

Related Work: Constrained RL uses the Constrained MDP (CMDP) to maximize a reward function subject to expected cost constraints (Satija, Amortila, and Pineau 2020; Pankavaraj and Varakantham 2023; Achiam et al. 2017; Gattami, Bai, and Aggarwal 2021; Tessler, Mankowitz, and Mannor 2018; Liang, Que, and Modiano 2018; Chow et al. 2018; Simão, Jansen, and Spaan 2021; Stooke, Achiam, and Abbeel 2020; Liu et al. 2022; Yu, Xu, and Zhang 2022; Zhang, Vuong, and Ross 2020). WCSAC (Yang et al. 2021) extends Soft Actor-Critic and considers a certain level of CVaR of the cost distribution as a safety measure; (Chow et al. 2017) use Lagrangian approach for the same. (Sootla et al. 2022) prevent only worst case cost (no CVaR or expected) violation by tracking the cost budget in the state, which further does not allow for multiple constraints. As far as we know and from benchmarking work (Ray, Achiam, and Amodei 2019), there is no constrained RL designed for long-horizon tasks, and even for short-horizon all current approaches need retraining if the constraint threshold changes.

Hierarchical Reinforcement Learning (HRL) addresses the problem of sequential decision making at multiple levels of abstraction (Kulkarni et al. 2016; Dietterich 2000). The problem could be formulated with the framework of MDP and semi-MDP (SMDP) (Sutton, Precup, and Singh 1999). Utilizing off-policy RL algorithms, a number of recent methods such as HIRO (Nachum et al. 2018), HRAC (Zhang et al. 2020), and HIGL (Kim, Seo, and Shin 2021) propose a hierarchy where both lower and upper level are RL learners and the higher level specifies sub-goals (Kaelbling 1993) for the lower level. However, it is hard to add safety constraints to such HRL with RL at both levels because to enforce constraints the higher level policy must generate constraint thresholds for the lower-level agent while ensuring the budget used by multiple invocations of the lower-level agent does not exceed the total cost budget. Also, the lowerlevel policy should be able to maximize reward for any given cost threshold in the different invocations by the upper level. However, both these tasks are not realizable with the existing results in constrained RL. Options or skills learning coupled with a higher level policy of choosing options is another approach (Eysenbach et al. 2018; Kim, Ahn, and Bengio 2019) in HRL. CoSHRL can be viewed as learning primitive skills of reaching local goals, and the simplicity of this task as well as of the search makes our approach scalable and flexible.

Closer to our method, SORB (Eysenbach, Salakhutdinov, and Levine 2019) employs a graph-based path-planning (Dijkstra's algorithm) at the higher level and distributional RL at low level, where the continuous state is discretized to yield a massive graph. SORB achieves better success rate in complex maze environments compared to other HRL techniques but cannot enforce constraint and has high computational cost due to a large graph. We present a thorough comparison of our ConstrainedRRT* to SORB's planner in Section 2. PALMER (Beker, Mohammadi, and Zamir 2022) employs

RRT* for the high level, but instead of distributional RL at the low-level it uses an offline RL like approach, requiring a large pre-collected dataset fully covering the environment; importantly, PALMER also cannot enforce constraints.

Logic based compositional RL (Jothimurugan et al. 2021; Neary et al. 2022) shares similarities with our approach in terms of combining a high-level planner with a low-level RL agent. However, works in compositional RL have a binary logical specification of success, whereas we are in a quantitative setting of constrained MDP with rewards and cost constraints (and novel CVaR constraints). Also, our utilization of the RRT* planner is quite different from the reachability planner used in these works.

Problem Formulation

We have an agent interacting with an environment in a Markov Decision Process (MDP) setting. The agent observes its current state $s \in S$, where $S \subset \mathbb{R}^d$ is a continuous state space. The initial state s_O for each episode is sampled according to a specified distribution and the agent seeks to reach goal state s_G . The agent's action space can be continuous ($a \subset \mathbb{R}^n$) or discrete. The episode terminates when the agent reaches the goal, or after T steps, whichever occurs first. The agent earns immediate reward $r^t(s^t, a^t)$ and separately also incurs immediate $\cos t^t(s^t, a^t)$ when acting in time step t. $V^\pi(s_O, s_G)$ and $V^\pi_c(s_O, s_G)$ are the cumulative undiscounted expected reward and cost respectively for reaching goal state s_G from origin state s_G following policy π . The typical optimization in constrained RL (Achiam et al. 2017) is:

$$\max_{\pi} V^{\pi}(s_O, s_G) \quad s.t. \quad V_c^{\pi}(s_O, s_G) \le K$$
 (1)

where the value functions are given as $V^{\pi}(s_O, s_G) = \mathbb{E}\left[\sum_{t=0}^T r^t(s^t, a^t)|s^T = s_G, s^0 = s_O\right]$ and $V^{\pi}_c(s_o, s_G) = \mathbb{E}\left[\sum_{t=0}^T c^t(s^t, a^t)|s^T = s_G, s^0 = s_O\right]$ with the expectation taken over policy and environment.

However, in the above, the constraint on the expected cost value is not always suitable to represent constraints on safety. E.g., to ensure that an autonomous electric vehicle is not stranded on a highway, we need a robust constraint that ensures the chance of that happening is low, which cannot be enforced by expected cost constraint. Therefore, we consider a cost constraint where we require that the CVaR (Rockafellar, Uryasev et al. 2000) of the cost distribution (given by the bold font random variable $\mathbf{V}_c^r(s_O, s_G)$ is less than a threshold. We skip writing s_O, s_G when implied. Intuitively, Value at Risk, VaR_α represents the minimum value for which the chance of violating the constraint (i.e., $\mathbf{V}_c^\pi > k$) is less than α specified as

$$VaR_{\alpha}(\mathbf{V}_{c}^{\pi}) = \inf\{k \mid Pr(\mathbf{V}_{c}^{\pi} > k) \leq \alpha\}$$

Conditional VaR, $CVaR_{\alpha}$ intuitively refers to the expectation of values that are more than the VaR_{α} , i.e., $CVaR_{\alpha}(\mathbf{V}_{c}^{\pi}) = \mathbb{E}[\mathbf{V}_{c}^{\pi} \mid \mathbf{V}_{c}^{\pi} \geq VaR_{\alpha}(\mathbf{V}_{c}^{\pi})]$. With this robust variant of the cost constraint (also known as percentile constraint), the problem that we solve for any given α is

$$\max_{\pi} V^{\pi}(s_O, s_G)$$
 s.t. $CVaR_{\alpha}(\mathbf{V}_c^{\pi}) \leq K$ (2)
Note that $\alpha = 1$ is risk neutral, i.e., $CVaR_1(\mathbf{V}_c^{\pi}) = \mathbb{E}[\mathbf{V}_c^{\pi}] = V_c^{\pi}$, and α close to 0 is completely risk averse.

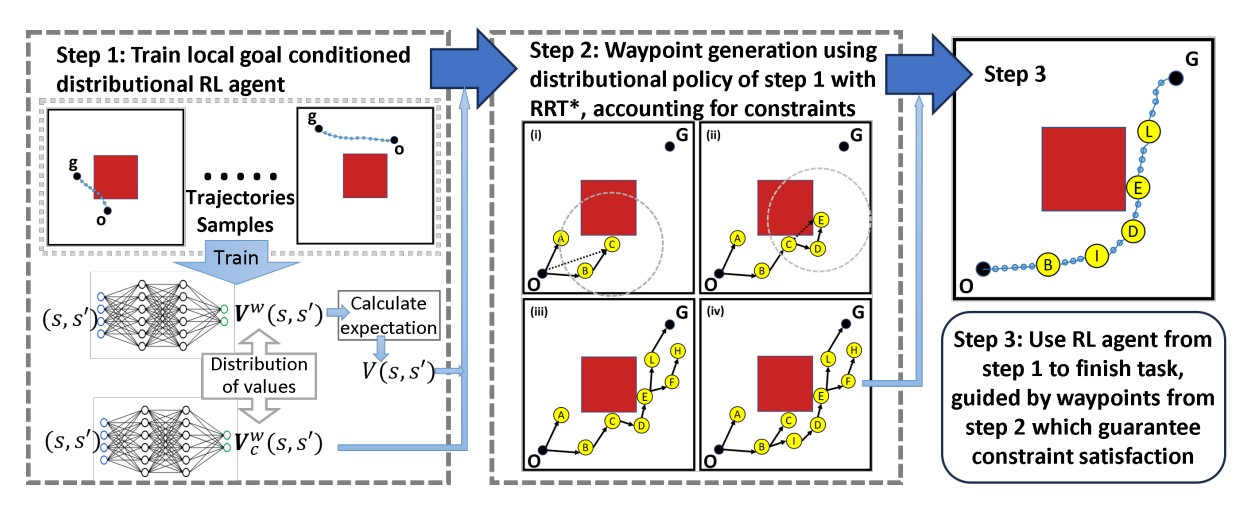


Figure 1: Overview of CoSHRL. **Step 1**: Train a local goal-conditioned RL agent using multiple randomly selected (o, g) (o is start, g is goal) pairs in a constrained environment (top part). The red square indicates a high-cost region. The learning is local and hence the goal will be unreachable if it's not "near" to the start. In this step, the local value function V and the cost function V_c are learned. **Step 2**: Generate waypoints guided by V and V_c using the proposed ConstrainedRRT* algorithm (i) The search samples state C, and O is not within the dashed circle of "near" states. Although both A and B are within the circle, the path from O to C via B is better as V(O,B) + V(B,C) < V(O,A) + V(A,C) using low-level agent's V function. So, edge (B, C) is added to the tree. (ii) For new sample E, E is "near" from C and D, but the edge (C, E) is not valid because of cost constraint $CVaR_{\alpha}(V_c(O,B) + V_c(B,C) + V_c(C,E)) > K$. (iii) A path (O, B, C, D, E, L, G) within the cost constraint is found. (iv) As the number of sampled states increases, a better path (O, B, I, D, E, L, G) is found. **Step 3**: Leveraging the waypoints from step 2, the pre-trained goal-conditioned RL agent completes the task.

2 Approach

Our approach, referred to as CoSHRL, solves the problem in Equation 2. As shown in Figure 1, CoSHRL employs a lower-level distributional RL agent and an upper-level search agent. First, the goal-conditioned (Kaelbling 1993) off-policy distributional RL agent learns local distribution of reward and cost between states that are "near" to each other. Then, the upper-level agent is constructed using a constrained search algorithm by utilizing the reward and cost distributions. Finally, through its interactions with the environment, the lower-level agent reaches the far away goal guided by the waypoints produced by the constrained search. Lower Level Agent: Distributional RL (Bellemare, Dabney, and Rowland 2023) is a popular technique that enables learning distribution of value functions instead of just expected values. Distributional RL learns a policy $\hat{\pi}$ and maintains a network representing the distribution of Q; we show how to derive \mathbf{V}, \mathbf{V}_c from the learned policy $\hat{\pi}$.

Why distributional RL? For rewards, we need to estimate just the expected $V^{\pi}(s,s')$, but it is known from the literature that learning the distribution of \mathbf{V}^{π} and then calculating expected value leads to better estimates (Eysenbach, Salakhutdinov, and Levine 2019; Beker, Mohammadi, and Zamir 2022). For completeness, we provide experimental evidence of this phenomenon in Appendix. For enforcing percentile based cost constraint, we need to estimate the distribution of cost \mathbf{V}_c for the $\hat{\pi}$ learned by lower-level agent. This is only possible with the use of distributional RL.

Representation: In distributional RL for discrete actions, the distribution of \mathbf{Q} is assumed to be over N discrete values. The distribution of a goal conditioned \mathbf{Q} is repre-

sented by Q^{θ} (neural network parameterized by θ), which takes as input s, s', a (s' is local goal) and outputs a vector $[p_1, \ldots, p_N]$ where p_i is the probability of expected reward value taking the i^{th} discrete value. For completeness, the standard training of distributional RL is described in the Appendix, yielding a trained policy $\hat{\pi}$. For training, we choose nearby start and end states at random throughout the state space, relying on the generalizability of neural networks to obtain good estimates for nearby start and goal in the whole state space.

Next, for discrete actions, we represent the distribution of value $\mathbf{V}^{\hat{\pi}}$ as a neural network V^w , which again outputs a probability vector. For simplicity, we do not include the learned policy $\hat{\pi}$ (which will not change) in the notation for V^w . The fixed learned $\hat{\pi}$ allows us to estimate V^w directly by minimizing the KL divergence between a target $V^t(s,s')=Q^\theta(s,s',a),a\sim\hat{\pi}(\cdot|s,s')$ and the current V^w , i.e., $\min_w D_{KL}(V^t||V^w)$. We optimize the above by storing experiences sampled according to $\hat{\pi}$ in a replay buffer and sampling mini-batches to minimize the loss above, analogous to supervised learning. Once the vector of probabilities V^w is obtained, we can obtain the expected V by calculating the expectation.

For continuous actions, we can directly learn the distribution of \mathbf{V} , represented by a network V^w using the same vector of probability representation of the distribution of value as used above for Q^θ .

For problems in path search with no movement uncertainty, reward r is set to -1 for each step such that the learned expected negated reward value function -V(s,s') reflects the estimated length of the shortest path (avoiding

impenetrable obstacles) from s to s' as done in (Kaelbling 1993; Eysenbach, Salakhutdinov, and Levine 2019). In particular, we assume that -V is learned accurately and prove the following result:

Lemma 1. Given $S \subset \mathbb{R}^d$, assuming -V gives the obstacle avoiding shortest path length, -V is a distance metric.

Next, for costs, we note that we performed the reward estimation without considering costs since in our approach the lower-level agent does not enforce constraints. However, the lower level agent does estimate the local costs as distributional ${\bf Q}$ values as a Q_c^θ network in the discrete action case or distributional ${\bf V}$ values as a V_c^w network in the continuous action case. Then, in the discrete action case, similar to above learning of V^w , the fixed learned policy $\hat{\pi}$ allows us to estimate the vector of probability V_c^w function directly by minimizing the KL divergence between a target $V_c^t = Q_c^\theta(s,s',a), a \sim \hat{\pi}(\cdot|s,s')$ and the current V_c^w : $\min_w D_{KL}(V_c^t||V_c^w)$. In the continuous action case, the network V_c^w is already learned directly (details in Appendix).

Upper Level Agent: Once the lower-level RL training is complete, we obtain a *local* goal-conditioned value function for any origin and local goal state that are near to each other. In this section, we use the learned expected value V and cost random variable V_c (removing superscripts for notation ease). First, we formulate the upper-level optimal constrained search problem. The RRT* search works in a continuous space $S \subset \mathbb{R}^d$. A path is a continuous function $\sigma: [0,1] \to \mathbb{R}^d$ with the start point as $\sigma(0)$ and end as $\sigma(1)$. In practice, a path is represented by a discrete number of states $\{\sigma(x_i)\}_{i \in [n]}$ for $0 = x_0 < x_1 < ... < x_{n-1} < x_n = 1$ and some positive integer n (n can be different for different paths). A collision-free path is one that has no overlap with fixed obstacles. The set of all paths is Σ , and the set of obstacle free paths is Σ_{free} . A length of path is defined as $\sup_{n:0=t_0 < ...t_n=1} \sum_{i=1}^n d(x_{t_{i-1}}, x_{t_i})$ for given underlying distance d. The RRT* search (or the Informed version) finds the shortest path from the given start and end point.

Given the discrete representation, for our CoSHRL the path traversed between $\sigma(x_i)$ and $\sigma(x_{i+1})$ is determined by the lower-level agent's policy. Every path $\sigma \in \Sigma$ provides a reward R_{σ} and incurs a cost C_{σ} . We define the reward for segment $(\sigma(x_i), \sigma(x_{i+1}))$ of a path as $V(\sigma(x_i), \sigma(x_{i+1}))$, where V is the local goal-conditioned value function learned by the lower-level agent. Similarly, the cost incurred for segment $(\sigma(x_i), \sigma(x_{i+1}))$ is $\mathbf{V}_c(\sigma(x_i), \sigma(x_{i+1}))$. Thus,

$$R_{\sigma} = \sum_{i=0}^{n-1} V(\sigma(x_i), \sigma(x_{i+1}))$$
(3)

$$\mathbf{C}_{\sigma} = \sum_{i=0}^{n-1} \mathbf{V}_c(\sigma(x_i), \sigma(x_{i+1})) \tag{4}$$

In CoSHRL, the constrained search problem is to find the optimal path, σ^* ($\in \operatorname{argmax}_{\sigma \in \Sigma} R_{\sigma}$) from s_O to s_G subject to a cost threshold, i.e., $CVaR_{\alpha}(\mathbf{C}_{\sigma^*}) \leq K$. As -V is the shortest distance considering obstacles (see the text before Lemma 1), the above optimization essentially finds the shortest path measured in distance -V from s_O to s_G avoiding all obstacles and within the cost constraint K.

```
Algorithm 1: ConstrainedRRT* (s_o, s_G, V, \mathbf{V}_c, K)
 1 \mathcal{V} \leftarrow \{s_o\}, \mathcal{E} \leftarrow \emptyset, S_{soln} \leftarrow \emptyset, \mathcal{T} = (\mathcal{V}, \mathcal{E})
 2 for iteration = 1 \dots N do
        \mathcal{T} = \mathsf{Extend\_node}(s_o, s_G, V, \mathbf{V}_c, K, \mathcal{T}, S_{soln})
 4 return best solution in S_{soln}
      def Extend_node (s_o, s_G, V, \mathbf{V}_c, K, \mathcal{T}, S_{soln})
                Sample s_{new} within \min(r_{RRT*}, \eta) from its
                  nearest node in \mathcal{T} as in Informed RRT*
                S_{near} \leftarrow \text{Find all nodes in } \mathcal{T} \text{ within }
               \min(r_{RRT*}, \eta) \text{ from } s_{new} Find s_{min} \in \operatorname{argmin}_s\{-R(s) - V(s, s_{new}) \mid s \in S_s^{rew}\}
               S_{near}, \text{Valid\_edge}(\mathcal{T}, s, s_{new}, \mathbf{V}_c, K)\}
\mathcal{V} \leftarrow \mathcal{V} \cup \{s_{new}\}, \mathcal{E} \leftarrow \mathcal{E} \cup \{(s_{min}, s_{new})\}
S_{cand} = \{s \in S_{near} \mid -R(s_{new}) - V(s_{new}, s) < -R(s), \text{Valid\_edge}(\mathcal{T}, s_{new}, s, \mathbf{V}_c, K)\}
               for \forall s \in S_{cand} do
10
                         \begin{array}{l} s_{parent} \leftarrow \text{Parent}(s), \mathcal{E} \leftarrow \mathcal{E} \backslash \{(s_{parent}, s)\}, \\ \mathcal{V} \leftarrow \mathcal{V} \cup \{s_{new}\}, \mathcal{E} \leftarrow \mathcal{E} \cup \{(s_{new}, s)\} \end{array} 
11
               If s_{new} is near the goal s_G, then form \sigma by
                  tracking parents of s_{new} and S_{soln} \leftarrow S_{soln} \cup \{\sigma\}
```

Our approach has immediate advantages over the state-of-the-art SORB (Eysenbach, Salakhutdinov, and Levine 2019), which also employs an upper level planner and lower level RL. SORB constructs a complete graph and then computes the shortest path using Dijkstra's algorithm. However, SORB has fundamental limitations: (1) The graph is built from the replay buffer of explored nodes. This can result in bad distribution of nodes in the state space (without considering start, goal, or obstacles). (2) The coarse discretization can result in a non-optimal path between the start and goal state (Karaman and Frazzoli 2011). (3) Construction of complete graph yields $O(N^2)$ complexity for Dijkstra's algorithm with N nodes (compared to $N \log N$ for our search).

Thus, an online search method that samples and grows a tree from the given start to the goal state while avoiding extending into obstacles is more suited as the upper-level search. Hence we provide Constrained-RRT*, which builds on Informed-RRT* (Gammell, Srinivasa, and Barfoot 2014) to handle constraints. Informed-RRT* builds upon RRT* (Karaman and Frazzoli 2011), which works by constructing a tree whose root is the start state and iteratively growing the tree by randomly sampling new points as nodes till the tree reaches the goal. In Informed RRT*, as an informed heuristic, the sampling is restricted to a *specially constructed ellipsoid*. However, both Informed-RRT* and RRT* do not take constraints into account.

Algorithm Description: We propose Constrained RRT* (Algorithm 1), which builds on Informed RRT* to handle the cost constraint. The pseudocode is provided in Algorithm 1. We search for the optimal path σ^* by incrementally building a tree $\mathcal T$ in the state space S. The tree, $\mathcal T$ consists of a set of nodes, $\mathcal V \ (\subset S)$, and edges $\mathcal E \ (\subset S \times S)$. In the subroutine Extend_node, a candidate state s_{new} is chosen (line 5) to be added to the tree $\mathcal T$ by a sampling process that is the same as in Informed RRT* (see Appendix for details of sam-

Algorithm 2: Valid_edge $(\mathcal{T}, s, s', \mathbf{V}_c, K)$

```
1 result \leftarrow \mathbf{V}_c(s,s')

2 while s.parent do

3 | result \leftarrow result + \mathbf{V}_c(s.parent,s)

4 | s \leftarrow s.parent

5 if CVaR_{\alpha}(result) \leq K then

6 |  return True

7 return False
```

pling). The hyper-parameter η accounts for the fact that our distance estimates are precise only locally (see Appendix for hyperparameter settings).

The rewiring radius, $r_{RRT*} = \gamma_{RRT*} (\log n/n)^{1/d}$, where n is the current number of nodes sampled, is described in (Karaman and Frazzoli 2011). The node s_{min} (line 7) that results in the shortest path (highest reward) to s_{new} among the nearby nodes S_{near} (line 6) is connected to s_{new} in line 8, if the edge is valid.

Here, we take a detour to explain how we determine the validity of edges. An edge is valid if and only if adding it does not result in a (partial) path that violates the cost constraint. The key insight is that this validity can be determined by computing the convolution of the distributions associated with the (partial) path and the current \mathbf{V}_c . By providing the definition of Valid_edge ($\mathcal{T}, s, s', \mathbf{V}_c, K$) in Algorithm 2 and doing the Valid_edge checks in the Extend_node subroutine, we ensure that any path output by the overall algorithm will satisfy the cost constraints. In the pseudocode of Valid_edge, \mathbf{V}_c represents a random variable (and so does result). Then, the addition in line 3 of Valid_edge is a convolution operation (recall that the distribution of a sum $\mathbf{X} + \mathbf{Y}$ of two random variables \mathbf{X}, \mathbf{Y} is found by a convolution (Ross 2014)).

Coming back to Extend_node, we explore further the possible edges to be added to the tree. In particular, in line 9 (1) the edge is created only if it is valid and (2) new edges are created from s_{new} to vertices in S_{near} , if the path through s_{new} has lower distance (higher reward) than the path through the current parent; in this case, the edge linking the vertex to its current parent is deleted, to maintain the tree structure. An example search run is shown in Figure 1.

Theoretical Results: The RRT* algorithm (Karaman and Frazzoli 2011) satisfies two properties: *probabilistic completeness* and *asymptotic optimality*. Intuitively, probabilistic completeness says that as number of samples $n \to \infty$, RRT* finds a feasible path if it exists and asymptotic optimality says that as $n \to \infty$, RRT* finds the optimal path with the highest reward. Unsurprisingly, asymptotic optimality implies probabilistic completeness. Our key contribution is proving asymptotic optimality of ConstrainedRRT*, which requires complicated analysis because of constraints.

Background: We summarize many definitions from Karaman and Frazzoli (2011). For detailed definition statements, we request the reader to peruse the referred paper. Karaman and Frazzoli (2011) define addition and multiplication operations that make the set of paths Σ a vector space. Further, they define a norm $||\sigma||_{BV}$ on this vector space (please re-

fer to page 22 of (Karaman and Frazzoli 2011)). The distance induced by the BV norm allows for defining limits of a sequence of path, i.e., $\lim_{n\to\infty}\sigma_n$. A solution path σ^* is called *robustly optimal* if under the metric induced by the BV norm for any sequence of collision-free paths σ_n , if $\lim_{n\to\infty}\sigma_n=\sigma^*$ then $\lim_{n\to\infty}R_{\sigma_n}=R_{\sigma^*}$. A path is said to have *strong* δ *clearance* if it is not within δ distance of any obstacle. A path σ has weak δ clearance if there exists a sequence of paths with strong clearance converging to σ . For any path finding algorithm ALG, let Y_n^{ALG} be the random variable corresponding to the reward of the max-reward solution returned at the end of iteration n.

Definition 1 (Asymptotic optimality (Karaman and Frazzoli 2011)). *An algorithm ALG is asymptotically optimal if, for any path search problem that admits a robustly optimal solution with finite reward* R^* , $\mathbb{P}(\{\limsup_n Y_n^{ALG} = R^*\}) = 1$.

Theoretical Results for Constraints: In this paper, due to the presence of constraints, we have to modify definitions. For instance, robustly optimal definition has to account for costs, i.e., the solution path σ^* is called *robustly optimal with* constraints if under the metric induced by the BV norm for any sequence of collision-free paths σ_n if $\lim_{n\to\infty} \sigma_n = \sigma^*$ then $\lim_{n\to\infty}R_{\sigma_n}=R_{\sigma^*}$ and if $\lim_{n\to\infty}\sigma_n=\sigma^*$ then $\lim_{n\to\infty}C_{\sigma_n}=C_{\sigma^*}$. Next, the definition of weak δ clearance of optimal path σ^* is extended to assume that there exists a sequence of strong δ clearance paths with total cost $\leq K + \epsilon$ when the path σ^* has cost $\leq K$ for any small $\epsilon > 0$. Intuitively, this means that if the optimal path has cost at most K then nearby strong δ clearance paths converging to the optimal path are also cost bounded closely by K while allowing ϵ extra cost for possibly slightly longer paths. We redefine Definition 1 with the cost constraint. Let Z_n^{ALG} be the random variable corresponding to the cost of the max-reward solution included in the graph returned by ALG at the end of iteration n (n samples). Then, we define:

Definition 2 (Asymptotic optimality with constraints). An algorithm ALG is asymptotically optimal with constraints if, for any path search problem that admits a robustly optimal solution with finite cost constraints K and with finite reward R^* , $\mathbb{P}(\{\limsup_n Y_n^{ALG} = R^*\}) = 1$ and $Z_n^{ALG} \leq K$.

We justify this definition as follows: since ALG will stop in finite n, we require that the output of ALG is always within the cost threshold K for any n at which the algorithm stops. We prove that our change (Valid_Edge check) preserves asymptotic optimality with constraints.

Theorem 1. Let d be the dimension of the space S, $\mu(S_{free})$ denotes the Lebesgue measure (i.e., volume) of the obstacle-free space, and τ_d be the volume of the unit Euclidean norm ball in the d-dimensional space. The Constrained RRT* in Algorithm 1 preserves asymptotic optimality with constraints for $\gamma_{RRT*} \geq (2(1+1/d))^{1/d} \left(\frac{\mu(S_{free})}{\tau_d}\right)^{1/d}$.

The proof of RRT* involves constructing a random graph via a marked point process that is shown as equivalent to the RRT* algorithm. In the full proof in Appendix. we incorporate cost constraints in the construction of the random graph and show its equivalence to ConstrainedRRT*. Then, the analysis is done for this constructed random graph. The

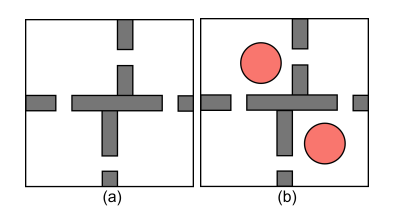


Figure 2(a): The complex point maze environment. Wall obstacles are in black. The environment on the right has hazardous red circles.

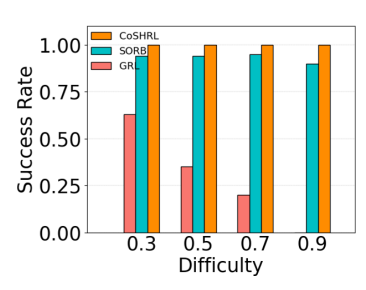


Figure 2(b): Success rate vs Difficulty

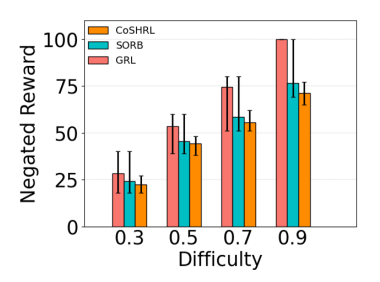


Figure 2(c): Neg. reward vs Difficulty

analysis involves (1) constructing a sequence of paths σ_n with strong δ_n clearance converging to the optimal path σ^* within cost constraint, (2) constructing a covering of the path σ_n with a sequence of norm balls with radius $\delta_n/4$; we use a special value for δ_n to account for cost constraints. It is shown that with large enough n and our special choice of δ_n , the tree in ConstrainedRRT* will have a path satisfying cost constraints through these balls and will converge to σ^* .

3 Experiments

We evaluate our method on two complex point maze environments and a novel image-based ViZDoom environment which have been used as a benchmark in RL navigation tasks (Zhang et al. 2020; Nachum et al. 2018; Beker, Mohammadi, and Zamir 2022). These maps include *obstacles* (impenetrable) and *hazards* (high cost but penetrable). We compare against SAC-Lagrangian (SAC-lag) (Yang et al. 2021; Stooke, Achiam, and Abbeel 2020), WCSAC (Yang et al. 2021), SORB (Eysenbach, Salakhutdinov, and Levine 2019), and Goal-conditioned RL (GRL) (Kaelbling 1993). SORB and GRL are not designed to enforce constraints, so they can get higher rewards but suffer from constraint violations. *Hyperparameter settings and additional results on other environments are in Appendix*.

2D Navigation with Obstacles: The first environment is point maze environment of Figure 2a (left), which has wall obstacles, but no hazards (thus, no cost constraints). The start point is randomly set in the environment while the goal is set 69ν away from the start where ν is the difficulty level. As the immediate reward r(s,a)=-1, the agent needs to reach the goal using the shortest path that avoids the walls.

We compare CoSHRL with goal-conditioned RL and SORB at different difficulty levels. For a fair comparison, both the number of nodes for SORB and the number of iterations for our method are set as 1000. For each experiment, we ran 100 trials with different seeds. We compare (a) the percentage of times the agent reaches the goal; and (b) the negated reward (i.e., the path length). In Figure 2b, we observe that the success rate of CoSHRL is 100% and it outperforms SORB with a larger margin as the difficulty level increases. In Figure 2c, we show all trials' negated reward (lower is better) for GRL, SORB, and CoSHRL. The difficulty level ν decides the optimal distance between start and goal, e.g., when $\nu=0.3$, the optimal distance is set at $69\times0.3\approx21$; we observed that the baseline approaches frequently provided very circuitous paths much longer than the

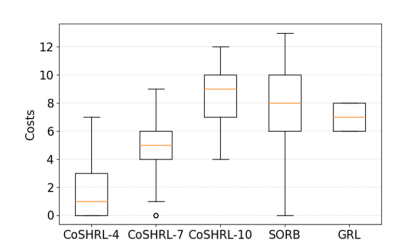
optimal path, e.g., SORB and GRL often provide circuitous paths with length exceeding 40 for $\nu=0.3$, so we cut them off at 40 for $\nu=0.3$. We cut all trajectories off for baselines (thereby providing advantage to baselines) at 40,60,80,100 for difficulty levels 0.3,0.5,0.7,0.9 respectively.

Yet, we observe that not only the average negated reward (path length) but also the upper bound and lower bound outperform SORB and GRL at different difficulty levels.

2D Navigation with Obstacles and Hazards: In this part, we evaluate our method in the point maze environment of Figure 2a (right), where there are two hazards set in the top left room and bottom left room. The agent starts randomly in the bottom left room and the goal is randomly set in the top right room. The trajectory length will be longer if the agent tries to avoid the hazardous area. We show results for static costs as well as for stochastic costs at different risk levels. It is worth noting that we don't need to retrain our lower-level RL policy for different cost thresholds K.

Static Cost: In this environment, the agent incurs a cost c=1for each step in the hazard, otherwise c=0. We evaluate our method with different cost limits K shown with CoSHRL-4, CoSHRL-7, and CoSHRL-10 in Figure 3b and Figure 3a. In Figure 3b, the bars provide the path length (negated reward) to reach the goal (plotted on the primary Y-axis) and the purple dots indicate the success rate (plotted on the secondary Y-axis). For average negated reward (path length), we only consider the successful trials for all algorithms. We have the following key observations from Figure 3b: (1) Our method reaches the goal with a high success rate under different cost limits with nearly 100% success. (2) Even though our method considers cost constraints, it is able to outperform SORB (which does not consider the cost constraint) not only in success rate but also in the length of the trajectory (average negated reward). (3) The success rate of GRL (goal-conditioned RL) is less than 20% but for the average negated reward we only count the successful trials, hence the negated reward for goal-conditioned RL is better (lower) than our method. (4) WCSAC and SAC-Lagrangian, both non-hierarchical RL techniques that consider cost constraints, have $\approx 0\%$ success rate in this long-horizon task and we don't consider them as baselines in further experiments.

The min., max. and mean cost for the different algorithms are shown in Figure 3a. With increasing cost limit, the upper bound, lower bound, and median of the total cost increase for CoSHRL. This is expected as the path in the hazardous area increases and therefore potentially the error in the computa-



static risk after training in maze environment. Only successful trials are counted for reward.

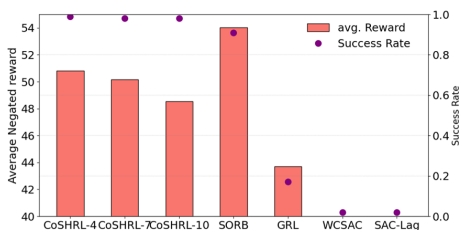
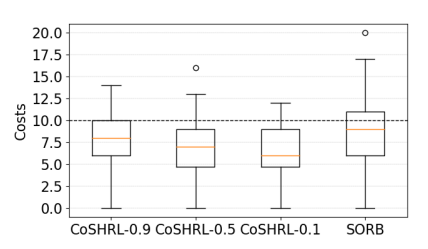


Figure 3(b): Success rate and avg. neg. reward of Figure 3(a): Boxplot of cost in evaluation for our method and baselines in maze environment. Figure 3(c): Boxplot of cost evaluation for



stochastic risk after training

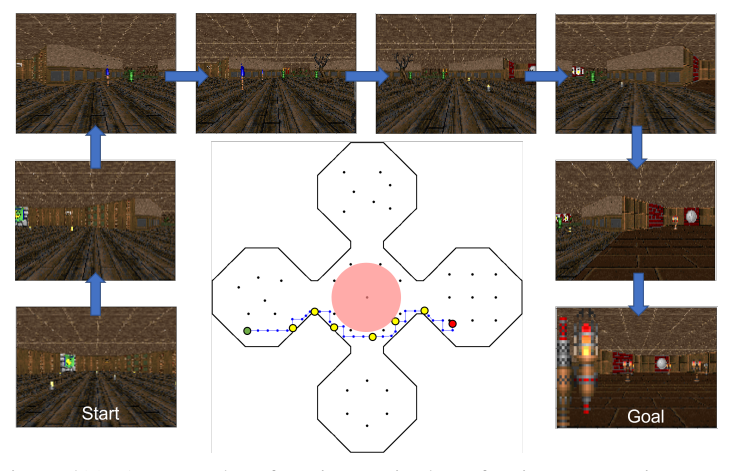


Figure 4(a): An example safe trajectory in the safe ViZDoom environment. Fixed obstacles are shown in black points and hazardous area is shown in red circle. Given a start state (green point) and goal state (red point), our method could find a sequence of waypoints (yellow points) conditioning on flexible constraints threshold K (K = 0 in this figure). Using the low level RL between the waypoints our method could reach the goal constraints (shown in the blue line).

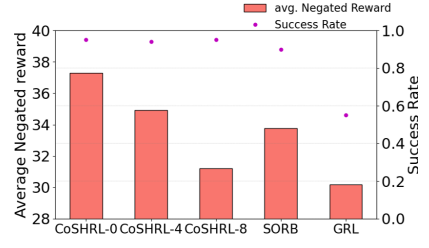


Figure 4(b): Success rate and avg. negated reward of our method, SORB, and GRL in Safe-ViZDoom. Only successful trials are counted for reward

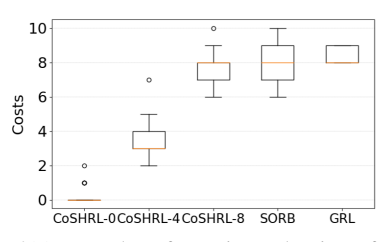


Figure 4(c): Boxplot of cost in evaluation after training in Safe-ViZDoom.

tion of V_c can increase. The proportion of trajectories that exceed the cost limit K=4,7,10 are 4%,6%,6% respectively. Examples of paths produced by different approaches are shown in Appendix.

Stochastic Cost: In this environment, the agent incurs a cost c uniformly sampled from $\{0, 1, 2\}$ for each step in the hazard, otherwise c = 0, i.e., the total cost of n steps inside the hazard follows a multinomial distribution. In safety-critical domains, a worst-case cost guarantee is preferred over the average cost bound (Yang et al. 2021). To achieve this, we use CVaR (Rockafellar, Uryasev et al. 2000) instead of the expected value of cost to threshold the safety of a policy.

We set cost limit K = 10 for all α , that is, the expectation of the cost of the worst $\alpha * 100\%$ cases should be lower than K. We evaluate our method with different α shown with CoSHRL-0.9, CoSHRL-0.5, and CoSHRL-0.1. All experiments are averaged over 100 runs.

In Table 1, the results show that our method CoSHRL with $\alpha = 0.9, 0.5$ satisfy the corresponding CVaR bound (columns $C\alpha$ shows the estimated average costs of the worst $\alpha * 100\%$ trajectories) while CoSHRL violates the CVaR bound (K=10) slightly with the tight level $\alpha=0.1$ because of the inherent approximation in distributional RL,

	EC	C0.9	C0.5	C0.1	ENR	%
CoSHRL-0.9	7.90	8.47	10.20	14.67	47.83	16%
CoSHRL-0.5	6.68	7.31	9.20	13.22	48.58	11%
CoSHRL-0.1	6.47	7.06	8.86	12.11	48.60	7%
SORB	8.06	8.97	11.54	15.14	52.98	30.5%

Table 1: Different metrics of performance in the environment with stochastic cost: expected cost (EC), cost-CVaR-0.9 (C0.9), cost-CVaR-0.5 (C0.5), cost-CVaR-0.1 (C0.1), and expected negated reward (ENR)

namely that of discretization and truncation of long-tailed multinomial distribution. As α decreases, our method is more risk-averse so the percentage of trajectories that exceed the cost limit K decreases (% column), and cost and reward both improve. The statistical properties of the total cost incurred by CoSHRL under different risk level α are shown in Figure 3c.

Image-based Navigation with Obstacles and Hazards: Due to the lack of a constrained image-based environment, we design the Safe-ViZDoom environment in Figure 4a based on ViZDoom (Wydmuch, Kempka, and Jaśkowski 2019). The Safe-VizDoom environment is a labyrinth in the shape of a clover with a hazardous area in the middle, making it challenging due to the very narrow safe area in the middle. The agent can move North/South/East/West by a fixed distance, whereas states only consist of first-person visual perspective (3x160x120 dimension). The agent incurs a cost c=1 for each step in the hazard, otherwise c=0. The start is randomly placed in one of the four rooms, while the goal is randomly set in the opposite room.

We evaluate CoSHRL with different cost limits K shown as CoSHRL-0, CoSHRL-4, and CoSHRL-8 in Figure 4b and Figure 4c without retraining the low level RL agent. Each result is the average over 100 random runs. We obtain similar results to other domains. Figure 4b shows that CoSHRL achieves a high success rate (> 95%) in reaching the goal with varying cost limits. As the cost limit increases, CoSHRL obtains shorter paths (avg. negated reward), indicating that the agent ventures deeper into hazards. For avg. negated reward, CoSHRL outperforms the unconstrained SORB and GRL for cost limit K=8, which is roughly the cost incurred by SORB and GRL in Figure 4c. Figure 4c shows the proportions of trajectories exceeding the cost limits of K=0,4,8 are 2%, 4%, 5% respectively. In comparison, unconstrained SORB and GRL achieve shorter path lengths (average negated reward) but incur cost over 8 in over half of their trajectories. The non-hierarchical GRL has a low success rate of 55%, resulting in the agent getting stuck in corners.

4 Discussion

We introduced a *constrained search* within the hierarchical RL approach. The RL agent is utilized to find paths between any two "nearby" states. Then, the constrained search utilizes the RL agent to reach far away goal states from starting states, while satisfying various types of constraints. We were able to demonstrate the better scalability, theoretical soundness, and empirical utility of our approach, CoSHRL, over existing approaches for Constrained RL and Hierarchical RL. Next, we discuss some limitations and future work.

Our work is based on the assumption that the low level RL agent has a high success rate in reaching each waypoint, even though there might be events such as action execution failure. RL in general can handle action execution uncertainty (process noise) by observing the current (unexpected) state after an action failure and appropriately executing contingency actions from such observations. Thus, the low level RL will ultimately reach the local goal even though it might occasionally (with some probability) take more steps due to action execution failure. In extreme cases, due to poor generalization the low level RL can declare a state unreachable, even though the state might be reachable. This can sometimes result in no path being found to the final goal. However, this happens very rarely, which is the main reason why the success rate of our method in the test environments (Figures 3b, 4b) are not exactly 100%. A possible direction to improve this is for constrained RRT* to actively ask for retraining the low level agent; an active retraining paradigm could be an interesting future research direction.

5 Acknowledgments

This research/project is supported by the National Research Foundation Singapore and DSO National Laboratories under the AI Singapore Programme (AISG Award No: AISG2-RP-2020-017)

References

Achiam, J.; Held, D.; Tamar, A.; and Abbeel, P. 2017. Constrained policy optimization. In *International conference on machine learning*, 22–31. PMLR.

Beker, O.; Mohammadi, M.; and Zamir, A. 2022. PALMER: Perception-Action Loop with Memory for Long-Horizon Planning. *arXiv preprint arXiv:2212.04581*.

Bellemare, M. G.; Dabney, W.; and Rowland, M. 2023. *Distributional Reinforcement Learning*. MIT Press. http://www.distributional-rl.org.

Chow, Y.; Ghavamzadeh, M.; Janson, L.; and Pavone, M. 2017. Risk-constrained reinforcement learning with percentile risk criteria. *The Journal of Machine Learning Research*, 18(1): 6070–6120.

Chow, Y.; Nachum, O.; Duenez-Guzman, E.; and Ghavamzadeh, M. 2018. A lyapunov-based approach to safe reinforcement learning. *Advances in neural information processing systems*, 31.

Dietterich, T. G. 2000. Hierarchical reinforcement learning with the MAXQ value function decomposition. *Journal of artificial intelligence research*, 13: 227–303.

Eysenbach, B.; Gupta, A.; Ibarz, J.; and Levine, S. 2018. Diversity is all you need: Learning skills without a reward function. *arXiv preprint arXiv:1802.06070*.

Eysenbach, B.; Salakhutdinov, R. R.; and Levine, S. 2019. Search on the replay buffer: Bridging planning and reinforcement learning. *Advances in Neural Information Processing Systems*, 32.

François-Lavet, V.; Henderson, P.; Islam, R.; Bellemare, M. G.; Pineau, J.; et al. 2018. An introduction to deep reinforcement learning. *Foundations and Trends® in Machine Learning*, 11(3-4): 219–354.

Gammell, J. D.; Srinivasa, S. S.; and Barfoot, T. D. 2014. Informed RRT*: Optimal sampling-based path planning focused via direct sampling of an admissible ellipsoidal heuristic. In 2014 IEEE/RSJ International Conference on Intelligent Robots and Systems, 2997–3004. IEEE.

Gattami, A.; Bai, Q.; and Aggarwal, V. 2021. Reinforcement learning for constrained markov decision processes. In *International Conference on Artificial Intelligence and Statistics*, 2656–2664. PMLR.

Hernandez-Leal, P.; Kartal, B.; and Taylor, M. E. 2019. A survey and critique of multiagent deep reinforcement learning. *Autonomous Agents and Multi-Agent Systems*, 33(6): 750–797.

Jothimurugan, K.; Bansal, S.; Bastani, O.; and Alur, R. 2021. Compositional reinforcement learning from logical specifications. *Advances in Neural Information Processing Systems*, 34: 10026–10039.

- Kaelbling, L. P. 1993. Learning to achieve goals. In *IJCAI*, volume 2, 1094–8. Citeseer.
- Karaman, S.; and Frazzoli, E. 2011. Sampling-based algorithms for optimal motion planning. *The international journal of robotics research*, 30(7): 846–894.
- Kim, J.; Seo, Y.; and Shin, J. 2021. Landmark-guided subgoal generation in hierarchical reinforcement learning. *Advances in Neural Information Processing Systems*, 34: 28336–28349.
- Kim, T.; Ahn, S.; and Bengio, Y. 2019. Variational temporal abstraction. *Advances in Neural Information Processing Systems*, 32.
- Kulkarni, T. D.; Narasimhan, K.; Saeedi, A.; and Tenenbaum, J. 2016. Hierarchical deep reinforcement learning: Integrating temporal abstraction and intrinsic motivation. *Advances in neural information processing systems*, 29.
- Levy, A.; Konidaris, G.; Platt, R.; and Saenko, K. 2017. Learning multi-level hierarchies with hindsight. *arXiv* preprint arXiv:1712.00948.
- Liang, Q.; Que, F.; and Modiano, E. 2018. Accelerated primal-dual policy optimization for safe reinforcement learning. *arXiv* preprint arXiv:1802.06480.
- Liu, M.; Zhu, M.; and Zhang, W. 2022. Goal-Conditioned Reinforcement Learning: Problems and Solutions. In Raedt, L. D., ed., *Proceedings of the Thirty-First International Joint Conference on Artificial Intelligence, IJCAI-22*, 5502–5511. International Joint Conferences on Artificial Intelligence Organization. Survey Track.
- Liu, Z.; Cen, Z.; Isenbaev, V.; Liu, W.; Wu, S.; Li, B.; and Zhao, D. 2022. Constrained variational policy optimization for safe reinforcement learning. In *International Conference on Machine Learning*, 13644–13668. PMLR.
- Nachum, O.; Gu, S. S.; Lee, H.; and Levine, S. 2018. Data-efficient hierarchical reinforcement learning. *Advances in neural information processing systems*, 31.
- Neary, C.; Verginis, C.; Cubuktepe, M.; and Topcu, U. 2022. Verifiable and compositional reinforcement learning systems. In *Proceedings of the International Conference on Automated Planning and Scheduling*, volume 32, 615–623.
- Pankayaraj, P.; and Varakantham, P. 2023. Constrained reinforcement learning in hard exploration problems. In *Proceedings of the AAAI Conference on Artificial Intelligence*, volume 37, 15055–15063.
- Ray, A.; Achiam, J.; and Amodei, D. 2019. Benchmarking safe exploration in deep reinforcement learning. *arXiv* preprint arXiv:1910.01708, 7: 1.
- Rockafellar, R. T.; Uryasev, S.; et al. 2000. Optimization of conditional value-at-risk. *Journal of risk*, 2: 21–42.
- Ross, S. M. 2014. *Introduction to probability models*. Academic press.
- Roza, F. S.; Roscher, K.; and Günnemann, S. 2023. Safe and Efficient Operation with Constrained Hierarchical Reinforcement Learning. In *Sixteenth European Workshop on Reinforcement Learning*.

- Satija, H.; Amortila, P.; and Pineau, J. 2020. Constrained markov decision processes via backward value functions. In *International Conference on Machine Learning*, 8502–8511. PMLR.
- Simão, T. D.; Jansen, N.; and Spaan, M. T. 2021. AlwaysSafe: Reinforcement learning without safety constraint violations during training. In *Proceedings of the 20th International Conference on Autonomous Agents and MultiAgent Systems*. International Foundation for Autonomous Agents and Multiagent Systems.
- Sootla, A.; Cowen-Rivers, A. I.; Jafferjee, T.; Wang, Z.; Mguni, D. H.; Wang, J.; and Ammar, H. 2022. Sauté rl: Almost surely safe reinforcement learning using state augmentation. In *International Conference on Machine Learning*, 20423–20443. PMLR.
- Stooke, A.; Achiam, J.; and Abbeel, P. 2020. Responsive safety in reinforcement learning by pid lagrangian methods. In *International Conference on Machine Learning*, 9133–9143. PMLR.
- Sutton, R. S.; Precup, D.; and Singh, S. 1999. Between MDPs and semi-MDPs: A framework for temporal abstraction in reinforcement learning. *Artificial intelligence*, 112(1-2): 181–211.
- Tessler, C.; Mankowitz, D. J.; and Mannor, S. 2018. Reward constrained policy optimization. *arXiv preprint arXiv:1805.11074*.
- Wydmuch, M.; Kempka, M.; and Jaśkowski, W. 2019. ViZ-Doom Competitions: Playing Doom from Pixels. *IEEE Transactions on Games*, 11(3): 248–259. The 2022 IEEE Transactions on Games Outstanding Paper Award.
- Yang, Q.; Simão, T. D.; Tindemans, S. H.; and Spaan, M. T. 2021. WCSAC: Worst-Case Soft Actor Critic for Safety-Constrained Reinforcement Learning. In *AAAI*, 10639–10646.
- Yu, H.; Xu, W.; and Zhang, H. 2022. Towards safe reinforcement learning with a safety editor policy. *Advances in Neural Information Processing Systems*, 35: 2608–2621.
- Zhang, T.; Guo, S.; Tan, T.; Hu, X.; and Chen, F. 2020. Generating adjacency-constrained subgoals in hierarchical reinforcement learning. *Advances in Neural Information Processing Systems*, 33: 21579–21590.
- Zhang, Y.; Vuong, Q.; and Ross, K. 2020. First order constrained optimization in policy space. *Advances in Neural Information Processing Systems*, 33: 15338–15349.